Partitioning of trace elements and metals between quasi-ultrafine, accumulation and coarse aerosols in indoor and outdoor air in schools

Viana M.[1]*, Rivas I.[1,2,3,4,7], Querol X.[1], Alastuey A.[1], Álvarez-Pedrerol M.[2,3,4], Bouso L.[2,3,4], Sioutas C.[6], Sunyer J.[2,3,4,5].

[1] Institute for Environmental Assessment and Water Research (IDAEA-CSIC), Barcelona, Spain.
[2] Centre for Research in Environmental Epidemiology (CREAL), Barcelona, Spain
[3] Universitat Pompeu Fabra (UFP), Barcelona, Spain.
[4] CIBER Epidemiología y Salud Pública (CIBERESP), Spain.
[5] Hospital del Mar Research Institute (IMIM), Barcelona, Spain.
[6] University of Southern California, Los Angeles, USA.
[7] Institut de Ciencia i Tecnologia Ambientals, Universitat Autonoma de Barcelona (UAB), Bellaterra Cerdanyola, Spain.
*Corresponding author: M. Viana (mar.viana@idaea.csic.es)

Abstract

Particle size distribution patterns of trace elements and metals across three size fractions (<0.25 µm, quasi-ultrafine particles, q-UF; 0.25-2.5 µm, accumulation particles; 2.5-10 µm, coarse particles) were analysed in indoor and outdoor air at 39 primary schools across Barcelona (Spain). Special attention was paid to emission sources in each particle size range. Results evidenced the presence in q-UF particles of high proportions of elements typically found in coarse PM (Ca, Al, Fe, Mn or Na), as well as several potentially health-hazardous metals (Mn, Cu, Sn, V, Pb). Modal shifts (e.g., from accumulation to coarse or q-UF particles) were detected when particles infiltrated indoors, mainly for secondary inorganic aerosols. Our results indicate that the location of schools in heavily trafficked areas increases the abundance of q-UF particles, which infiltrate indoors quite effectively, and thus may impact children exposure to these health-hazardous particles.

Keywords: infiltration; sources; metals and elements; ultrafine particles, UFP; $PM_{0.25}$.

Introduction

Most of the concern over atmospheric particles derives from their impact on a number of aspects, ranging from climate (Shindell et al., 2012) or visibility (Cheung et al., 2005), to human health (WHO, 2013). In regard to the latter, aerosol effects are dependent on particle size, with different health effects being associated to different particle diameters (WHO, 2013). Aerosols may be classified based on particle diameter as coarse (aerodynamic diameter >1 µm), fine (1 µm>aerodynamic diameter> 100 nm), ultrafine particles (<100 nm) and nanoparticles (<50 nm) (Seinfeld & Pandis, 1998). Some of these definitions may vary, especially for the finer size fractions (Kumar et al., 2010). Recent studies have extended the use of the term ultrafine particles to particles up to 250 nm in diameter, referring to this size fraction as “quasi-ultrafine” (Saffari et al., 2013).

Numerous studies have evidenced a wide range of adverse health outcomes on the human cardiovascular and respiratory systems linked to the exposure to airborne coarse, fine and ultrafine particles (Cassee et al., 2013). Whereas coarse aerosols impact mostly on respiratory system (Pérez et al., 2008), ultrafine particles have the ability to translocate to the circulatory system and induce inflammation (Oberdorster, 2001).

The partitioning of elements among various sizes depends on their sources and affects their chemical composition and therefore will impact the potential toxicity induced on different regions of the body (Cassee et al., 2013). Based on their chemical composition different types of particles generate reactive oxidative species, with metallic particles such as Cu and Fe being a well-known example (Fu et al., 2014) albeit not the only one (e.g., soluble and mineral particles; Hetland et al., 2001). Because literature results evidence that health effects from airborne particles depend on their chemical composition (e.g., transition metals, combustion-derived organic particles) but also

on physical properties (size, particle number; Cassee et al., 2013), it is essential to assess the link between the two by evaluating the concentration of major and trace aerosol components across particle size fractions. This assessment could be used as input data for the assessment of health effects of particles reaching different regions of the body.

In addition to health effects studies, source apportionment analyses of ultrafine particles and nanoparticles by receptor modelling tools also require chemical size distribution data. For coarse and fine aerosols, tracer elements of specific emission sources (e.g., vehicular traffic, mineral dust, sea salt, among others) are well established and have been frequently used in the literature (Bruinen de Bruin et al., 2006). However, studies have indicated that such tracers may not be common across particle size fractions (Lin et al., 2005; Miller et al., 2007; Gietl et al., 2010; Buonanno et al., 2011; Liati et al., 2012; Patel et al., 2012). As an example, whereas Al and Ca are known to be tracers of mineral dust in coarse aerosols, they may be derived from local-scale combustion processes when found in ultrafine particles (Lin et al., 2005). As a result, interpreting Al and Ca as tracers of mineral matter in ultrafine particles may be misleading for specific cases (Sanderson et al., 2014). Similar cases are reported for Fe, Ca, P and Mg in ultrafine particles from lubricating oils (Miller et al., 2007; Patel et al., 2012) and for Ca, Mg, Al and Fe in ultrafine particles from diesel soot (Liati et al., 2012; Sanderson et al., 2014). Consequently, relatively few source apportionment studies of ultrafine particles are currently available (Karanasiou et al., 2007; Sanderson et al, 2014).

Finally, understanding the way in which elements partition across particle size fractions also allows us to interpret changes in such particle size distributions, especially those induced by physical and/or chemical processes, such as particle infiltration from outdoor to indoor air. Infiltration processes may alter particle size distribution and aerosol composition for specific aerosols, e.g., volatilization of ammonium nitrate (Hering et al., 2007). The assessment of the chemical size distribution data of aerosol components should enhance our understanding of the extent to which infiltration processes affect indoor aerosols, and provide better insights on indoor exposures. In the present study, this analysis targets children and their exposure to indoor airborne pollutants during school hours. Previous studies on indoor air quality in schools (Blondeau et al., 2005; Diapouli et al., 2007; Weichenthal et al., 2008; Morawska et al., 2009; Mejía et al., 2011; Mazaheri et al., 2014) concluded that research on indoor air quality in typical schools is vital to students' health and their performance, given that numerous outdoor airborne pollutants are present in schools.

This work aims to quantify the distribution of major metals and trace elements across three particle size fractions in urban outdoor and indoor air. This assessment was carried out in primary schools in Barcelona, both indoors and outdoors, and at different distances from traffic emissions. Our results provide qualitative and quantitative descriptions of particle size distribution patterns for metals and trace elements, with a special focus on their emission sources in each particle size range.

Methodology

Sampling locations

Measurements were carried out in 39 schools across Barcelona (Spain), selected in the framework of the Advanced ERC Grant BREATHE. Schools were divided into those representative of the city's urban background pollution levels and of high traffic emissions (Rivas et al., 2014), and then grouped into pairs (one school of each type) for concurrent sampling. In each school, indoor and outdoor sampling was carried out simultaneously. Further details of the sampling locations are provided elsewhere (Rivas et al., 2014; Viana et al., 2014). Two six-month sampling campaigns took place between January 2012 and February 2013, at a rate of 2 schools per week. Sampling was carried out at each school twice.

Sample collection and analysis

Filter samples were collected using Personal Cascade Impactor Samplers (PCIS; Misra et al., 2002) connected to SKC Leland Legacy pumps, operating at 9 lpm. Four PCIS were placed

simultaneously (2 indoors, 2 outdoors) in each school. Samples were collected only during school hours (9:00-17:00 local time, 8 hours) over a period of 4 consecutive days (Monday to Thursday). Thus, samples accumulated 32 sampling hours on the same filters and were representative of weekly (4-day) school-hour concentrations.

Each PCIS collected size-fractionated particles in the size ranges <0.25 µm (quasi-ultrafine particles, q-UF), 0.25-2.5 µm (accumulation mode particles), and 2.5-10 µm (coarse PM). The collection substrates were Pall quartz-fibre filters (Pall Tissuquartz 2500QAT-UP), 25 mm in diameter for the coarse and accumulation stages, and 37 mm for q-UF particles.

After collection, mass concentrations were gravimetrically determined by weighing the filter substrates on a Mettler-Toledo Microbalance. All samples were then analysed for major and trace elements. For each school, week and environment (indoor and outdoor), 2 parallel samples (with 3 filter substrates each) were available: A and B. The mass concentration on samples A and B was comparable. The filters from PCIS A were acid digested (HNO_3:HF:$HClO_4$) to determine major and trace elements by ICP-MS and ICP-AES (Querol et al., 2001). The filters from PCIS B were cut in two halves: one half was leached in deionised water to extract the soluble fraction, which was analysed by ion chromatography and ion selective electrode to determine concentrations of SO_4^{2-}, NO_3^-, Cl^- and NH_4^+. The remaining half filter was used for determination of OC and EC by thermal-optical transmission (TOT) with a Sunset OCEC Analyzer following the temperature protocol NIOSH. This methodology was applied equally to each of the size ranges (q-UF, accumulation and coarse).

In total, the number of valid samples for outdoor air was 84 and 144 for sampling campaigns 1 and 2, respectively, and 75 and 126 for indoor air for sampling campaigns 1 and 2.

Results and discussion

Mean indoor and outdoor concentrations

The size-fractionated mean concentrations of major and trace components, as well as the gravimetrically determined mass, for indoor and outdoor air samples, are shown in Figure 1. The data shown are the mean concentrations for both sampling campaigns, and thus representative of cold and warm periods separately, and of the annual mean when combined. The measurements were taken during the school year (while children were inside the classrooms). The mass closure of indoor and outdoor aerosols is not described in detail, as it is not the main focus of this work. The mass closure for the first sampling campaign was discussed in detail in Viana et al. (2014), whereas this work focusses on particle size distribution patterns and across both sampling campaigns.

An initial assessment demonstrates larger differences between the mass of the three size fractions in indoor than in outdoor air, with a mass ratio between coarse and accumulation mode particles of 2.3 indoors and of 1.5 outdoors, respectively. This difference is mainly induced by the higher indoor organic carbon (OC) mass. In indoor air, OC was the major contributor to all size fractions, accounting for 74% of coarse, 80% of accumulation and 39% of q-UF particles. As described by Rivas et al (2014) and Viana et al (2014), the main origin of organic aerosols in indoor air in the schools under study was human activity (textiles, skin flakes, etc.). Also in indoor air, the second largest contributor to all size fractions were major elements Al_2O_3, Ca, Fe, K and Mg, most of them tracers of mineral matter in coarse and accumulation particles. In q-UF particles, the source origin of these major metals is most probably also mineral. However, in trace concentrations much lower than the ones obtained in this study, these elements may also originate from road dust (Dahl et al., 2006), traffic fuels (diesel or gasoline) and/or to lubricants, among others (Sanderson et al., 2014). It is also possible that the high contribution of mineral elements to q-UF particles is, to a certain extent, an effect of bounce-off from previous stages in the impactors, or to a slight deviation from the expected cut-off diameter due to flow control. This is a known limitation of impaction techniques (Gomes et al., 1990). However, Misra et al (2002) showed that bounce is negligible with PCIS

impactors due to the relatively low jet velocity (645 cm/s) in the 2.5 um stage. This potential artefact was not quantified in the present work.

Mineral elements accounted for 15% of coarse, 6% of accumulation and 9% of q-UF particles indoors. In coarse particles, the main source of mineral dust was re-suspension of indoor- and outdoor-originated dust within the classrooms (Amato et al., 2014; Rivas et al., 2014; Viana et al., 2014). The high contribution of mineral elements to q-UF particle mass (2.3 $\mu g/m^3$) was an unexpected result, given that mineral contributions are generally considered to be minimal in this size fraction (Seinfeld & Pandis, 1998). However, Rivas et al (2014) showed that the levels of mineral matter in $PM_{2.5}$ at the Barcelona schools are much higher than those measured in the Barcelona urban background. Tracers of marine aerosols (Na and Cl^-) contributed with 4-5% of particle mass across size fractions, although it should be stated that traces of Na could originate from other (anthropogenic) sources in q-UF particles, as in the case of other major elements (based on the low R^2 between Na and Cl^-, <0.3).

Relatively larger similarities were observed in the chemical composition of the different particle size fractions outdoors, when compared to indoor air. Organic matter was again the main contributor to all size fractions outdoors, with contributions ranging from 57% of coarse particles to 74% of accumulation and 30% of q-UF particles. The main source of outdoor carbonaceous aerosols (including elemental carbon, contributing with 1-5% of the PM mass) in the Barcelona schools under study was vehicular traffic (Amato et al., 2014). Mineral elements accounted for 13% of coarse, 5% of accumulation and 10% of q-UF particle mass, similarly to indoor air, even if in terms of mass concentration the contribution was higher indoors for coarse particles (5.6 $\mu g/m^3$ indoors *vs*. 2.7 $\mu g/m^3$ outdoors). As in the case of indoor air, the mineral mass in q-UF particles found outdoors (2.3 $\mu g/m^3$) was high, as observed also by Rivas et al. (2014) for $PM_{2.5}$. The mineral mass in q-UF particles was higher than that reported by Daher et al. (2013) for traffic-influenced sites in central Los Angeles (0.84 $\mu g/m^3$), suggesting the possibility of an additional source of q-UF mineral particles in the Barcelona schools. Saffari et al. (2013) also reported mineral matter concentrations lower than in Barcelona. These results, together with the higher organic mass indoors also in coarse particles (27.1 $\mu g/m^3$ indoors vs. 11.9 $\mu g/\mu m^3$ outdoors) confirm the high exposure of schoolchildren in Barcelona to mineral and organic aerosols reported in detail elsewhere (Rivas et al., 2014; Viana et al., 2014).

Partitioning of chemical components across particle size fractions

The particle size distribution patterns of major and trace elements are discussed in the following sections. Because only three size fractions are available, the terms “patterns” or “particle size distribution patterns” are used throughout the text, as opposed to “particle size distributions” which is more appropriate when a larger number of size channels is available. The terms “unimodal” or “bimodal” are only used on specific occasions.

a) Outdoor air

The mean distribution of major and trace elements in outdoor air are shown in Figure 2. The behaviour of each individual element and component was assessed in order to evaluate how they partition between size fractions, attempting to identify common patterns and to infer potential emission sources. Initially, the prevalence of mass concentrations in one or two modes was identified, but the distinction between them was at times not straightforward. In order to apply a systematic approach, an arbitrary threshold of 20% was defined as the minimum difference between mass concentrations to define a mode. As an example, for a given element, the ratio between the mass concentration in the coarse and accumulation modes was calculated, and also the ratio between q-UF and accumulation modes. If both ratios indicated mass differences between modes >20%, then the distribution was classified as having 2 modes, because there was a >20% mass difference between the coarse and accumulation modes, and between the q-UF and accumulation modes (“U” shaped distribution). Conversely, if only one ratio showed a mass difference >20% then the distribution was classified as having only 1 mode

Applying this classification scheme, the following patterns were identified (Figure 2 and Table 1):

One mode, with prevalence for accumulation particles (1A): as expected (Seinfeld & Pandis, 1998), this was the characteristic size distribution of NO_3^- aerosols in outdoor air. Because NO_3^- may be present in the form of NH_4NO_3 but also forming salts with coarser cations (Ca, Na, etc.), 46% of the mean NO_3^- mass was found in accumulation particles followed by 31% of the mass in coarse and 23% of the mass in q-UF particles. Despite showing 2 modes (Table 1), SO_4^{2-} and NH_4^+ are also described here due to their prevalence in the accumulation mode. Sulphate was found mostly in the form of $(NH_4)_2SO_4$ and therefore showed a strong contribution in the accumulation mode but also in q-UF particles (q-UF, 44%, and accumulation, 42%, classified as 2UA). The same pattern was followed by NH_4^+, with prevalence for accumulation (45% of the mass) and q-UF (43%) particles (pattern 2UA).

One mode, with prevalence for coarse particles (1C): components with this size distribution were Sb and Ga. This distribution suggests a single source for each of these species, or different sources emitting particles in the same size range. In the case of Sb, the emission sources are mostly linked to vehicular emissions (road dust re-suspension, Bruinen de Bruin et al., 2006), which generate coarse particles.

One mode, with prevalence for q-UF particles (1U): EC, Cr, Ni, Ge, Sr, Zr, Mo, Cd, Ba, La and Ce partitioned in this way. This group of species shows a clear link with anthropogenic emissions, specifically vehicular traffic (EC, Cd, Sr, Ba) and industrial emissions (Ni, Cr, Ge, Mo, Cd). These elements may be either emitted as primary q-UF particles or formed in the atmosphere as a result of nucleation from high-temperature vaporization processes, also possibly linked to vehicular traffic (Sanders et al., 2003).

Two modes (accumulation and coarse), with similar mass in both modes (2CA): OC aerosols followed this pattern, suggesting natural (bioaerosols) and anthropogenic (traffic, industry, background aerosols) sources. The fact that these species are more prevalent in the two coarser sized fractions (coarse and accumulation particles) suggests also the possibility of some atmospheric aging.

Two modes (coarse and q-UF), with prevalence for coarse particles (2Cu): components with higher mass in the coarse mode but also with significant mass in q-UF particles were Ca, Fe, Mg, Na, Li, Ti, Mn, Cu, Rb and Sn. This group of elements shows marked contributions from mineral tracers (Ca, Fe, Mg, Li, Ti, Mn, Rb) and sea salt (Na, Mg) in the coarse mode. Also, results evidence the presence in outdoor q-UF particles of typically mineral and sea salt-derived elements, and in relatively high proportions (e.g., 29% of Ca in q-UF particles, 33% of Fe, 37% of Mg or even 40% of Na, Table S1). In trace concentrations lower than the ones reported here, some of these elements may also be tracers of traffic when found in q-UF particles (Lin et al., 2005; Dahl et al., 2006; Patel et al., 2012; Sanderson et al., 2014). In coarse and q-UF particles, mineral matter components in the Barcelona schools may originate from city dust with additional contributions from local playground dust, which is finely ground by children's activities (Rivas et al., 2014). Regarding the trace metals in this group, the partitioning of some of them in coarse particles (Sn, Cu, Ti, Rb) may be expected as resulting from road dust re-suspension (Amato et al., 2009). In addition to mineral dust as a major contributor to q-UF particles, traces of these elements in q-UF particles could derive from road dust (Dahl et al., 2006), their use as additives in lubricant oils (Saffari et al., 2013) and/or from vaporisation of metals due to the high temperatures reached during the braking process (Sanders et al., 2003).

Two modes (coarse and q-UF), with similar mass in q-UF and coarse particles (2UC): only two components showed this pattern, Al_2O_3 and V, with a prevalence for q-UF particles although also with a significant contribution from coarse particles. In trace concentrations in q-UF particles, Al_2O_3 and V have been associated with combustion processes (Sanderson et al., 2014). However, the major origin of these elements in q-UF particles is probably mineral dust, from the school playgrounds and/or from road dust (Al_2O_3 and K; Dahl et al., 2006). In coarse particles, Al_2O_3 is

linked with mineral matter (Bruinen de Bruin et al., 2006), and fine V is associated with fuel-oil combustion (Tolocka et al., 2004).

Two modes (coarse and q-UF), with prevalence for q-UF particles (2Uc): K was the only element to follow this pattern, linked with mineral matter and biomass burning emissions in coarse particles and with mineral dust in q-UF particles.

b) Indoor air

Similar size distribution patterns were detected for indoor air (Table 1 and Figure 3):

One mode, with prevalence for coarse particles (1C): Sb and Ga followed the same pattern as outdoors, which was also followed indoors by NO_3^- and Cl^-. Indoor NO_3^- showed prevalence for coarse particles and lower absolute mass concentrations than outdoors (1.2 µg/m^3 outdoors *vs*. 0.4 µg/m^3 indoors), thus evidencing the evaporation of fine NO_3^- species during infiltration from outdoor to indoor air (Hering et al., 2007). In case of Cl^-, whereas no specific pattern was detected outdoors, indoors there was an enrichment in coarse particles (1.0 µg/m^3 outdoors *vs*. 1.2 µg/m^3 indoors), which could be related to Cl^- emissions from cleaning products, and a decrease in accumulation mode Cl^- (0.9 µg/m^3 outdoors *vs*. 0.7 µg/m^3 indoors). However, it should be noted that these concentration differences are low and close to the detection limits of the instruments.

One mode, with prevalence for q-UF particles (1U): as in outdoor air, EC, Ni, Ge, Mo and Cd followed this pattern, and also SO_4^{2-}. This group of species is associated with typical outdoor anthropogenic emissions (mainly from vehicular traffic and industrial emissions), which infiltrate indoors. The concentrations of accumulation mode SO_4^{2-} particles detected outdoors (pattern 2UA) seem to decrease indoors, whereas coarse SO_4^{2-} particle mass increases. The absolute mass is similar in indoor when compared to outdoor air for sulphate, and lower for the rest of the components analysed.

Two modes (coarse and q-UF), with prevalence for coarse particles (2Cu): components with prevalence for coarse particles but with a secondary q-UF particle mode in indoor air were Fe, Ca, Mg, Na, Li, Ti, Mn, Cu, Rb, Sn, Al_2O_3, V, As, Sr and Pb. The first (Fe, Ca, Mg, Na, Li, Ti, Mn, Cu, Rb, Sn) showed the same pattern outdoors, suggesting that at least one indoor source of these elements was infiltration from outdoor air. Given their mostly mineral origin, another indoor source would be re-suspension of indoor dust (originated indoors or entrained from playgrounds by the children). In the case of Ti, concentrations in the coarse mode were 80 ng/m^3 indoors and 55 ng/m^3 outdoors, whereas they were fairly similar in the q-UF and accumulation modes. This may indicate the presence of a specific indoor source of coarse Ti particles, which could be related to the re-suspension of settled particles of outdoor origin or to TiO_2 used as white pigment in paint (Uhde & Salthammer, 2007). For Ca, an additional enrichment in coarse particles indoors was detected, which results from the contribution from chalk dust (Rivas et al., 2014). Absolute indoor Ca concentrations were higher than outdoors by a factor of 2.6, especially in the coarse mode (I/O factor of 3.0). Mineral dust re-suspension and the subsequent enrichment in coarse particles was also the most probable cause for the modal shift observed for the remaining components in this group (Al_2O_3, V, As, Sr, Pb). Al_2O_3 followed a 2UC pattern outdoors and shifted to a coarse pattern (2Cu) indoors, due to an increase in the coarse Al_2O_3 mass. V followed a similar pattern, as it may substitute Al in crystalline structures. A similar increase in coarse Sr was detected in indoor air, together with a marked decrease in q-UF Sr with respect to outdoor air (where Sr followed a 1U pattern). Elements which may be less related to mineral matter (e.g., As) also showed increases in coarse mode mass and decreases in the masses of accumulation and q-UF particles in indoor with respect to outdoor air. Absolute concentrations were always similar or lower indoors.

As in the case of outdoor air, these results indicate the presence in q-UF particles in indoor air of typical tracers of mineral matter (both of indoor and outdoor origin), and in relatively high proportions (e.g., 35% of Al_2O_3, 17% of Ca, 21% of Fe, 39% of K, 24% of Mg or 27% of Na, Table S2). These results also show the presence in indoor air of trace and potentially toxic metals in q-UF particles, such as Mn, Cu, Sn, V or Pb. The origin of these metals is probably infiltration from

outdoor air. As a result, metallic q-UF particles are detected indoors and thus may impact exposure of schoolchildren.

Two modes (coarse and q-UF), with prevalence for q-UF particles (2Uc): only one element (Cr) was identified with a consistent and strong prevalence for q-UF particles and a smaller contribution in coarse particles.

Two modes (coarse and q-UF), with similar mass in both modes (2UC): a similar case to the 2Cu pattern, but with an even stronger enrichment in coarse particles, was detected for K, Zn, Ba, La and Ce. These elements showed a prevalence for q-UF particles in outdoor air (1U or 2Uc patterns), whereas indoors an increase in the absolute coarse mass concentration of all of them was detected. This suggests the presence of indoor sources (possibly, mineral), and the increased exposure of children to these elements in coarse aerosols.

Two modes (q-UF and accumulation), with similar mass in both modes (2UA): in indoor air, NH_4^+ was the only component to show this mass size distribution pattern. A similar pattern was expected for SO_4^{2-}, but however absolute concentrations were similar (1.2 μg/m^3 outdoors *vs*. 1.3 μg/m^3 indoors) but a shift toward q-UF particles was detected in indoor air (pattern 1U, Figure 3). This shift was relative and linked not with an increase of q-UF SO_4^{2-} but with a reduction in accumulation mode SO_4^{2-} (ratio I/O for accumulation particles = 0.7). This could be related to infiltration losses due to particle size, even though infiltration is known to be most efficient for particles in the accumulation mode (Long et al., 2001). In addition, an increase in coarse SO_4^{2-} particles was detected (ratio I/O for coarse particles = 2.2), which probably originate from indoor-specific sources such as chalk from blackboards (Rivas et al., 2014; Viana et al., 2014).

Two modes (accumulation and coarse), with similar mass in both modes (2CA): indoor OC followed the same pattern as in outdoor air, as a result of infiltration of outdoor particles indoors. In addition to the outdoor sources of OC described above, one additional source of coarse indoor OC (human activity, Rivas et al., 2014) contributed to an enhanced coarse OC mode, with a larger coarse/accumulation ratio (2.2 indoors *vs*. 1.1 outdoors).

In sum, typically mineral elements (e.g., Ca, Fe, Mg, Al, Ti, Sr) prevailed in coarse aerosols indoors due to the influence of indoor sources (dust re-suspension). In addition, exposure to metallic particles in the q-UF size mode was also evidenced (EC, Ni, Mo, Cd), which resulted mainly from outdoor infiltration. The presence of typically mineral elements in q-UF particles (e.g., Fe, Mg, Na, Li, Ti) was also shown in indoor air, probably sourcing from finely ground mineral matter from playgrounds (Rivas et al., 2014). During infiltration, secondary inorganic aerosols underwent a modal shift, towards coarse particles in the case of NO_3^- and towards q-UF particles in the case of SO_4^{2-}.

c) <u>Influence of road traffic</u>

A detailed analysis was carried out for schools located in high- and low-traffic areas of the city, as described in the Methodology section and by Rivas et al. (2014). This analysis was only carried out for outdoor air, aiming to avoid the influence of other variables such as infiltration.

When compared to the mean size distributions obtained for outdoor air, the results from the high traffic schools show a marked shift towards the finer grain-sized fractions, with most of the components evidencing at least one mode in the q-UF particle range (Table 1). This likely reflects the influence of fresh vehicular emissions, characterised by a higher fraction of ultrafine particles. On the other hand, at low traffic schools the prevailing size distributions were dominated by the accumulation mode, suggesting the transport and atmospheric ageing of fresh vehicular emissions towards urban background areas and the subsequent increase in particle size. Thus, the particle size of elements such as Cu, Fe or Rb which showed prevalence for coarse and q-UF particles (pattern 2Cu) at high traffic schools, shifted towards coarser particles only at low traffic schools (pattern 1C for Cu, and 1A for Fe and Rb). Similar cases were observed for elements such as Ca, Mg, Al or Pb. The number of elements showing prevalence for the coarse mode was higher at low

traffic with respect to high traffic schools (1C patterns for OC, NO_3^-, Cu, Se, Sn and Sb at low traffic schools *vs*. for Cl^- and Sb at high traffic schools). Results show that NO_3^- prevailed in the accumulation mode after oxidation from NOx emission in high traffic areas, and increased towards a coarse distribution after transport toward low traffic areas. Sulphate aerosols, on the other hand, showed maximum mass concentrations in q-UF and accumulation particles at high traffic schools, and shifted toward a unimodal q-UF pattern after ageing by means of a decrease in accumulation mode particles which probably shifted towards the coarse mode, as shown by the relative increase in coarse SO_4^{2-} particles (0.22 µg/m^3 in high-traffic *vs*. 0.35 in low traffic schools). Because the size distribution of particles outdoors influences indoor air quality through infiltration processes, our results evidence that the location of schools in heavily trafficked areas of the city has an impact on the amount of q-UF particles with the potential to infiltrate indoors, and thus on the increased exposure of schoolchildren to health-hazardous q-UF particles. This result supports the implementation of actions to reduce traffic emissions around schools.

d) Influence of seasonality

The variability in particle size of secondary organic and inorganic species (OC, SO_4^{2-}, NO_3^-) was assessed as a function of seasonality. This variability, induced by outdoor ambient temperature, should have an impact on indoor particles of outdoor origin through infiltration and thus on indoor exposure. To this end, mean outdoor ambient temperatures were calculated for each school and for the period Monday through Thursday, from 9-17h (school hours). Two types of scenarios were then identified: warm periods, with mean outdoor ambient temperature equal to or >20ºC (classified as “summer”; mean daily temperature 23.1ºC with 2.2ºC standard deviation), and cold periods with ambient temperatures <20ºC (“winter”; mean daily temperature 13.5ºC with 3.5ºC standard deviation). In total, 23 summer and 53 winter scenarios were analysed.

In outdoor air, the particle size patterns obtained for secondary inorganic aerosols followed expectations (Seinfeld & Pandis, 1998). In winter, under lower ambient temperatures, which favour the thermal stability of NH_4NO_3, NO_3^- concentrations peaked in the accumulation mode and thus NO_3^- was mostly present in this form (Figure 4). Under higher summer temperatures, NH_4NO_3 (accumulation mode) decomposed and coarser NO_3^- species (e.g., Ca or $NaNO_3$) were formed. Sulphate, on the other hand, did not undergo such a modal shift but the influence of higher summer temperatures was evidenced as an increase in absolute accumulation mode SO_4^{2-} concentrations (mostly $(NH_4)_2SO_4$) due to the higher oxidation rate of SO_2 (Hidy et al., 1994).

The particle sizes and concentrations of outdoor secondary inorganic aerosols influenced indoor air (Figure 4). Indoor NO_3^- followed a similar although less pronounced pattern than outdoors, with prevalence for accumulation particles (NH_4NO_3) in winter and for coarse particles (e.g., calcium/sodium NO_3^-) in summer. As expected, concentrations were lower indoors than outdoors in winter, when outdoor concentrations reached their annual maxima, with the largest reduction being observed for q-UF and accumulation particles in indoor air (outdoor/indoor ratios of 5.1-5.7 for q-UF and accumulation particles *vs*. of 3.1 for coarse particles). Therefore outdoor ambient temperatures seem to modify the particle size distribution patterns for NO_3^- aerosols outdoors, and that the same patterns were followed by NO_3^- indoors.

Sulphate aerosols, on the other hand, evidenced different patterns indoors as a function of outdoor temperatures. In outdoor air throughout the year, and indoors in summer, SO_4^{2-} was mostly present in accumulation and q-UF particles as expected. However, in indoor air and in winter, a decrease in accumulation SO_4^{2-} particles was consistently detected, which remains unexplained with the data available. This effect seems to be related with seasonality, as it was only detected in winter, and it is possibly related with infiltration given that the windows remain closed in winter. I/O ratios >1 were obtained in summer and winter for coarse SO_4^{2-} ($CaSO_4$), as a result of indoor emissions from blackboard chalk and the high mineral dust re-suspension (Rivas et al., 2014).

Finally, organic aerosols were also assessed, showing prevalence for accumulation and coarse particles in outdoor air (ratios >1.6 for accumulation and coarse over q-UF particles). In indoor air, particle size distribution patterns seemed to be more strongly influenced by indoor sources than by

seasonality. Both in winter and summer, indoor OC prevailed in coarse particles originating from human activity as described in the previous sections. Indoor concentrations were higher in winter due to the fact that windows were kept closed. In summer the absolute concentrations of q-UF and accumulation OC particles were similar to outdoor air because windows remained open most of the time, while coarse OC particles were higher indoors (ratio I/O = 1.4). This evidences that, as expected, OC emissions from human activity are mainly coarse.

Conclusions

This work aimed to describe particle size distribution patterns of major metals and trace elements in indoor and outdoor air in Barcelona, with a special focus on their emission sources in each particle size range. The main conclusions extracted may be summarised as follows:

- Mineral and typically coarse elements (e.g., Ca, Fe, Al, Mg, Na) were detected in relatively high proportions in indoor and outdoor q-UF particles (20-40% of their mass in q-UF). These elements originate mainly from mineral matter and sea salt, and they may also source in trace concentrations from anthropogenic emissions in particles <100 nm. The presence in indoor air of potentially toxic metals in q-UF particles (Mn, Cu, Sn, V, Pb) was also detected, with a potential impact on child exposure.
- Secondary inorganic aerosols, which prevailed in accumulation particles outdoors, evidenced modal shifts (NO_3^- towards coarse particles due to evaporation losses, and SO_4^{2-} towards q-UF particles due to the loss of accumulation particles) after they infiltrated indoors. The influence of an indoor-specific source of coarse sulphate was detected.
- At high traffic schools, size distribution patterns were dominated by q-UF particles reflecting the influence of fresh vehicular emissions. At low traffic schools, accumulation particles prevailed suggesting the transport of fresh vehicular emissions from high traffic areas. Our results demonstrate that the location of schools in heavily trafficked areas increases the amount of q-UF particles with the potential to infiltrate indoors, and thus impacts child exposure to health-hazardous q-UF particles. It is recommended that actions to reduce traffic emissions around schools should be undertaken.
- Outdoor ambient temperatures modified the particle size distribution patterns for NO_3^- aerosols outdoors, and the same patterns were followed by NO_3^- indoors. Sulphate, on the other hand, displayed different patterns indoors with respect to outdoors as a function of seasonality. The particle size distribution patterns for organic carbon in indoor air seemed to be more strongly influenced by emission sources than by seasonality.

Acknowledgements

The research leading to these results has received funding from the European Research Council under the ERC Grant Agreement number 268479 – the BREATHE project. Additional funding for specific instrumentation was provided by national project IMPACT (CGL2011-26574), the Spanish Ministry of Agriculture, Food and the Environment (UCA2009020083), and projects VAMOS (CLG2010-19464-CLI) and GRACCIECSD2007-00067. Support is acknowledged to Generalitat de Catalunya 2009 SGR8. The authors are indebted to the schools Antoni Brusi, Baloo, Betània – Patmos, Centre d'estudis Montseny, Col·legi Shalom, Costa i Llobera, El Sagrer, Els Llorers, Escola Pia de Sarrià, Escola Pia Balmes, Escola Ramon Llull, Escola Nostra Sra. de Lourdes, Escola Tècnica Professional del Clot, Ferran i Clua, Francesc Macià, Frederic Mistral, Infant Jesús, Joan Maragall, Jovellanos, La Llacuna del Poblenou, Lloret, Menéndez Pidal, Nuestra Señora del Rosario, Miralletes, Ramon Llull, Rius i Taulet, Pau Vila, Pere Vila, Pi d'en Xandri, Projecte, Prosperitat, Sant Ramon Nonat - Sagrat Cor, Santa Anna, Sant Gregori, Sagrat Cor Diputació, Tres Pins, Tomàs Moro, Torrent d'en Melis, and Virolai.

References

Amato, F., Pandolfi, M., Escrig, A., Querol, X., Alastuey, A., Pey, J., Perez, N., Hopke, P.K., 2009. Quantifying road dust resuspension in urban environment by Multilinear Engine: a comparison with PMF2. Atmos. Environ. 43, 2770–2780.

Amato, F., Rivas, I., Viana, M., Moreno, T., Bouso, L., Reche, C., Àlvarez-Pedrerol, M., Sunyer, J., Querol, X., 2014. Source apportionment of PM2.5 concentrations measured at 39 primary schools in Barcelona. Sci. Total Environ. submitted.

Blondeau P, Iordache V, Poupard O, Genin D, Allard F., 2005. Relationship between outdoor and indoor air quality in eight French schools. Indoor Air, 15, 2–12.

Bruinen de Bruin, Y., Koistinen, K., Yli-Tuomi, T., Kephalopoulos, S., Jantunen, M., 2006. A review of source apportionment techniques and marker substances available for identification of personal exposure, indoor and outdoor sources of chemicals. JRC - European Commission.

Buonanno, G., Stabile, L., Avino, P., Belluso, E., 2011. Chemical, dimensional and morphological ultrafine particle characterization from a waste-to-energy plant. Waste Manag. 31, 2253–62.

Cassee, F.R., Héroux, M.-E., Gerlofs-Nijland, M.E., Kelly, F.J., 2013. Particulate matter beyond mass: recent health evidence on the role of fractions, chemical constituents and sources of emission. Inhal. Toxicol. 25, 802–812.

Cheung, H.C., Wang, T., Baumann, K., Guo, H., 2005. Influence of regional pollution outflow on the concentrations of fine particulate matter and visibility in the coastal area of southern China. Atmos. Environ. 39, 6463–6474.

Dahl, A., Gharibi, A., Swietlicki, E., Gudmundsson, A., Bohgard, M., Ljungman, A., Blomqvist, G., Gustafsson, M., 2006. Traffic-generated emissions of ultrafine particles from pavement–tire interface. Atmos. Environ. 40, 1314–1323.

Diapouli, E., Chaloulakou, A., Spyrellis, N., 2007. Levels of ultrafine particles in different microenvironment- Implications to children exposure. Science of the Total Environment, 388, 128-136.

Fu, P.P., Xia, Q., Hwang, H.-M., Ray, P.C., Yu, H., 2014. Mechanisms of nanotoxicity: Generation of reactive oxygen species. J. Food Drug Anal. 1–12.

Gietl, J.K., Lawrence, R., Thorpe, A.J., Harrison, R.M., 2010. Identification of brake wear particles and derivation of a quantitative tracer for brake dust at a major road. Atmos. Environ. 44, 141–146.

Gomes, L., Bergametti, G., Dulac, F., Ezat, U., 1990. Assessing the actual size distribution of atmospheric aerosols collected with a cascade impactor. J. Aerosol Sci. 21, 47–59.

Hering, S. V, Lunden, M.M., Thatcher, T.L., Kirchstetter, T.W., Brown, N.J., 2007. Using regional data and building leakage to assess indoor concentrations of particles of outdoor origin. Aerosol Sci. Technol. 41, 639–654.

Hetland, R.B., Myhre, O., Låg, M., Hongve, D., Schwarze, P.E., Refsnes, M., 2001. Importance of soluble metals and reactive oxygen species for cytokine release induced by mineral particles. Toxicology 165, 133–44.

Karanasiou, A., Sitaras, I., Siskos, P., Eleftheriadis, K., 2007. Size distribution and sources of trace metals and n-alkanes in the Athens urban aerosol during summer. Atmos. Environ. 41, 2368–2381.

Kumar, P., Robins, A., Vardoulakis, S., Britter, R., 2010. A review of the characteristics of nanoparticles in the urban atmosphere and the prospects for developing regulatory controls. Atmos. Environ. 44, 5035–5052.

Liati, A., Dimopoulos Eggenschwiler, P., Müller Gubler, E., Schreiber, D., Aguirre, M., 2012. Investigation of diesel ash particulate matter: A scanning electron microscope and transmission electron microscope study. Atmos. Environ. 49, 391–402.

Lin, C.-C., Chen, S.-J., Huang, K.-L., Hwang, W.-I., Chang-Chien, G.-P., Lin, W.-Y., 2005. Characteristics of Metals in Nano/Ultrafine/Fine/Coarse Particles Collected Beside a Heavily Trafficked Road. Environ. Sci. Technol. 39, 8113–8122.

Long, C.M., Suh, H.H., Catalano, P.J., Koutrakis, P., 2001. Using Time- and Size-Resolved Particulate Data To Quantify Indoor Penetration and Deposition Behavior. Environ. Sci. Technol. 35, 2089–2099.

Mazaheri, M., Clifford, S., Jayaratne, R., Azman, M., Mokhtar, M., Fuoco, F., Buonanno, G., Morawska, L., 2014. School Children's Personal Exposure to Ultrafine Particles in the Urban Environment. Environmental Science and Technology, 48, 113-120.

Mejía, J. F., Choy, S. L., Mengersen, K. and Morawska, L., 2011. Methodology for assessing exposure and impacts of air pollutants in school children: Data collection, analysis and health effects – A literature review, Atmospheric Environment, 45(4), 813–823, doi:10.1016/j.atmosenv.2010.11.009.

Miller, A.L., Stipe, C.B., Habjan, M.C., Ahlstrand, G.G., 2007. Role of Lubrication Oil in Particulate Emissions from a Hydrogen-Powered Internal Combustion Engine. Environ. Sci. Technol. 41, 6828–6835.

Misra, C., Singh, M., Shen, S., Sioutas, C., Hall, P.M., 2002. Development and evaluation of a personal cascade impactor sampler (PCIS). J. Aerosol Sci. 33, 1027–1047.

Morawska, L., He, C., Johnson, G., Guo, H., Uhde, E., Ayoko, G., 2009. Ultrafine particles in indoor air of a school: possible role of secondary organic aerosols. Environmental Science and Technology, 15; 43(24):9103-9. doi: 10.1021/es902471a.

Oberdorster, G., 2001. Pulmonary effects of inhaled ultrafine particles. Int Arch Occup Env. Heal. 1–8.

Patel, M., Azanza Ricardo, C.L., Scardi, P., Aswath, P.B., 2012. Morphology, structure and chemistry of extracted diesel soot—Part I: Transmission electron microscopy, Raman spectroscopy, X-ray photoelectron spectroscopy and synchrotron X-ray diffraction study. Tribol. Int. 52, 29–39.

Pérez, L., Tobias, A., Querol, X., Künzli, N., Pey, J., Alastuey, A., Viana, M., Valero, N., González-Cabré, M., Sunyer, J., 2008. Coarse Particles From Saharan Dust and Daily Mortality. Epidemiology 19, 800–807.

Querol, X., Alastuey, A., Rodríguez, S., Plana, F., Ruiz, C.R., Cots, N., Massagué, G., Puig, O., 2001. PM10 and PM2.5 source apportionment in the Barcelona Metropolitan Area, Catalonia, Spain. Atmos. Environ. 35, 6407–6419.

Rivas, I., Viana, M., Moreno, T., Pandolfi, M., Amato, F., Reche, C., Bouso, L., Àlvarez-Pedrerol, M., Alastuey, A., Sunyer, J., Querol, X., 2014. Child exposure to indoor and outdoor air pollutants in schools in Barcelona. Environ. Int. submitted.

Saffari, A., Daher, N., Shafer, M.M., Schauer, J.J., Sioutas, C., 2013. Seasonal and spatial variation of trace elements and metals in quasi-ultrafine (PM0.25) particles in the Los Angeles metropolitan area and characterization of their sources. Environ. Pollut. 181, 14–23.

Sanders, P.G., Xu, N., Dalka, T.M., Maricq, M.M., 2003. Airborne brake wear debris: size distributions, composition, and a comparison of dynamometer and vehicle tests. Environ. Sci. Technol. 37, 4060–4069.

Sanderson, P., Delgado-Saborit, J.M., Harrison, R.M., 2014. A review of chemical and physical characterisation of atmospheric metallic nanoparticles. Atmos. Environ. in press.

Seinfeld, J.H., Pandis, S.N., 1998. Atmospheric Chemistry and Physics: From air pollution to climate change. John Wiley & Sons, Inc.

Shindell, D., Kuylenstierna, J.C.I., Vignati, E., van Dingenen, R., Amann, M., Klimont, Z., Anenberg, S.C., Muller, N., Janssens-Maenhout, G., Raes, F., Schwartz, J., Faluvegi, G., Pozzoli, L., Kupiainen, K., Höglund-Isaksson, L., Emberson, L., Streets, D., Ramanathan, V., Hicks, K., Oanh, N.T.K., Milly, G., Williams, M., Demkine, V., Fowler, D., 2012. Simultaneously mitigating near-term climate change and improving human health and food security. Science 335, 183–9.

Sunyer, J., Esnaola, M., Alvarez-Pedrerol, M., Rivas, I., Forns, J., Foraster, M., Garcia-Esteban, R., Basagaña, X., Viana, M., Cirac, M., Moreno, T., Alastuey, A., Sebastian, N., Nieuwenhuijsen, M., Quero, X., 2014. The negative effects of traffic related air pollution in school on cognitive function growth. N. Engl. J. Med. submitted.

Uhde, E., Salthammer, T., 2007. Impact of reaction products from building materials and furnishings on indoor air quality—A review of recent advances in indoor chemistry. Atmos. Environ. 41, 3111–3128.

Viana, M., Rivas, I., Querol, X., Alastuey, A., Sunyer, J., Álvarez-Pedrerol, M., Bouso, L., Sioutas, C., 2014. Indoor/outdoor relationshipsand mass closure of quasi-ultrafine, accumulation and coarse mode particles in Barcelona schools. Atmos. Chem. Phys. in press.

Weichenthal, S., Dufresne, A., Invante-Rivar, C., Joseph, L., 2008. Characterizing and predicting ultrafine particle counts in Canadian classrooms during the winter months: Model development and evaluation. Environmental Research, 106, 349-360.
WHO, 2013. Review of evidence on health aspects of air pollution – REVIHAAP Project. World Health Organization, Copenhagen.

Figure captions

Figure 1. Size-fractionated mean concentrations of major species, metals and trace components, as well as the gravimetrically determined mass, for indoor and outdoor air. Number of valid samples: 228 for outdoor air and 201 for indoor air.

Figure 2. Examples of size distribution patterns identified for outdoor air. The specific patterns for all the components analysed are shown in Figure S1 in Supporting Information. The patterns (in red, top left corner) are defined as follows: one mode, with prevalence for q-UF particles (1U); one mode, with prevalence for accumulation particles (1A); one mode, with prevalence for coarse particles (1C); two modes (coarse and q-UF), with prevalence for coarse particles (2Cu); two modes (coarse and q-UF), with prevalence for q-UF particles (2Uc); two modes (coarse and q-UF), with similar mass in both modes (2UC); two modes (q-UF and accumulation), with similar mass in both modes (2UA); two modes (accumulation and coarse), with similar mass in both modes (2CA).

Figure 3. Examples of size distribution patterns identified for indoor air. Specific patterns for all components are shown in Figure S2 in Supporting Information.

Figure 4. Particle size distribution patterns identified for secondary organic and inorganic species as a function of seasonality.

Table 1. Mean particle size distribution patterns identified in outdoor and air, as well as for outdoor air at schools with high and low traffic contributions. Pattern “0” indicates concentrations in the three particle size modes which were not significantly different from each other (within 20% margin).

Outdoor		Indoor		High Traffic (Outdoor)		Low Traffic (Outdoor)
NO_3^-	1A	Sb	1C	NO_3^-	1A	Al_2O_3
Ga	1C	Ga	1C	Cl^-	1C	Fe
Sb	1C	NO_3^-	1C	Sb	1C	Mg
EC	1U	Cl^-	1C	EC	1U	Na
Ni	1U	EC	1U	V	1U	Li
Ge	1U	Ni	1U	Ge	1U	Ti
Mo	1U	Ge	1U	As	1U	V
Cd	1U	Mo	1U	Se	1U	Mn
Sr	1U	Cd	1U	Sr	1U	Ni
Cr	1U	SO_4^{2-}	1U	Mo	1U	Rb
Ba	1U	Ca	2Cu	Cd	1U	Sr
La	1U	Fe	2Cu	Ca	2Cu	La
Ce	1U	Mg	2Cu	Fe	2Cu	Ce
Ca	2Cu	Na	2Cu	Mg	2Cu	OC
Fe	2Cu	Li	2Cu	Na	2Cu	NO_3^-
Mg	2Cu	Ti	2Cu	Ti	2Cu	Cu
Na	2Cu	Mn	2Cu	Mn	2Cu	Se
Li	2Cu	Cu	2Cu	Cu	2Cu	Sn
Ti	2Cu	Rb	2Cu	Rb	2Cu	Sb
Mn	2Cu	Sn	2Cu	Sn	2Cu	SO_4^{2-}
Cu	2Cu	Al_2O_3	2Cu	Al_2O_3	2Uc	NH_4^+
Rb	2Cu	V	2Cu	K	2Uc	Ca
Sn	2Cu	As	2Cu	Cr	2Uc	Pb
K	2Uc	Sr	2Cu	Ni	2Uc	EC
NH_4^+	2UA	Pb	2Cu	Ba	2Uc	K
SO_4^{2-}	2UA	Cr	2Uc	La	2Uc	Cr
Al_2O_3	2UC	K	2UC	Ce	2Uc	Ge
V	2UC	Zn	2UC	SO_4^{2-}	2UA	Ba
OC	2CA	Ba	2UC	Li	2UC	Mo
		La	2UC	P	2UC	Cd
		Ce	2UC	OC	2AC	
Cl^-	0	NH_4^+	2UA	NH_4^+	2AU	
P	0	OC	2CA	Pb	2AU	Cl^-
Sc	0					P
Co	0					Sc
Zn	0	P	0	Sc	0	Co
As	0	Sc	0	Co	0	Zn
Se	0	Co	0	Zn	0	Ga
Pb	0	Se	0	Ga	0	As

*Patterns: one mode, with prevalence for q-UF particles (1U); one mode, with prevalence for accumulation particles (1A); one mode, with prevalence for coarse particles (1C); two modes (coarse and q-UF), with prevalence for coarse particles (2Cu); two modes (coarse and q-UF), with prevalence for q-UF particles (2Uc); two modes (coarse and q-

UF), with similar mass in both modes (2UC); two modes (q-UF and accumulation), with similar mass in both modes (2UA); two modes (accumulation and coarse), with similar mass in both modes (2CA).

665 **Supporting Information**

666

667 Table S1. Mean mass distribution of major and trace elements in q-UF, accumulation and coarse
668 particles, in outdoor air.

669

	Outdoor		
	q-UF	**Accumulation**	**Coarse**
OC	23%	36%	40%
EC	64%	23%	13%
Al_2O_3	48%	11%	41%
Ca	29%	11%	59%
Fe	33%	9%	58%
K	48%	18%	35%
Mg	37%	11%	53%
Na	40%	7%	52%
SO_4^{2-}	44%	42%	14%
NO_3^-	23%	46%	31%
Cl^-	29%	33%	38%
NH_4^+	43%	45%	12%
Li	38%	14%	47%
P	36%	26%	38%
Sc	34%	32%	34%
Ti	30%	13%	57%
V	38%	29%	33%
Cr	82%	5%	13%
Mn	37%	13%	50%
Co	33%	33%	34%
Ni	87%	6%	7%
Cu	27%	20%	53%
Zn	35%	33%	31%
Ga	33%	29%	38%
Ge	95%	2%	3%
As	36%	33%	30%
Se	36%	33%	31%
Rb	32%	16%	53%
Sr	55%	22%	23%
Mo	96%	2%	2%
Cd	47%	29%	23%
Sn	35%	22%	43%
Sb	9%	12%	79%
Ba	64%	8%	28%
La	51%	14%	35%
Ce	60%	6%	34%
Pb	35%	35%	30%

670

671

Table S2. Mean mass distribution of major and trace elements in q-UF, accumulation and coarse particles, in indoor air.

	Indoor		
	q-UF	**Accumulation**	**Coarse**
OC	20%	25%	55%
EC	53%	23%	24%
Al_2O_3	35%	6%	59%
Ca	17%	14%	68%
Fe	21%	9%	69%
K	39%	17%	45%
Mg	24%	5%	71%
Na	27%	16%	57%
SO_4^{2-}	43%	28%	28%
NO_3^-	22%	34%	45%
Cl^-	28%	26%	45%
NH_4^+	46%	43%	11%
Li	15%	12%	74%
P	32%	25%	43%
Sc	32%	32%	35%
Ti	19%	11%	71%
V	30%	24%	45%
Cr	64%	15%	20%
Mn	25%	12%	63%
Co	30%	32%	38%
Ni	72%	16%	12%
Cu	32%	16%	51%
Zn	35%	23%	42%
Ga	28%	26%	46%
Ge	95%	3%	2%
As	31%	22%	47%
Se	36%	30%	34%
Rb	18%	14%	68%
Sr	19%	8%	73%
Mo	97%	2%	2%
Cd	44%	31%	25%
Sn	34%	19%	47%
Sb	9%	10%	81%
Ba	47%	6%	47%
La	43%	13%	44%
Ce	47%	5%	48%
Pb	33%	22%	45%

Figure 1

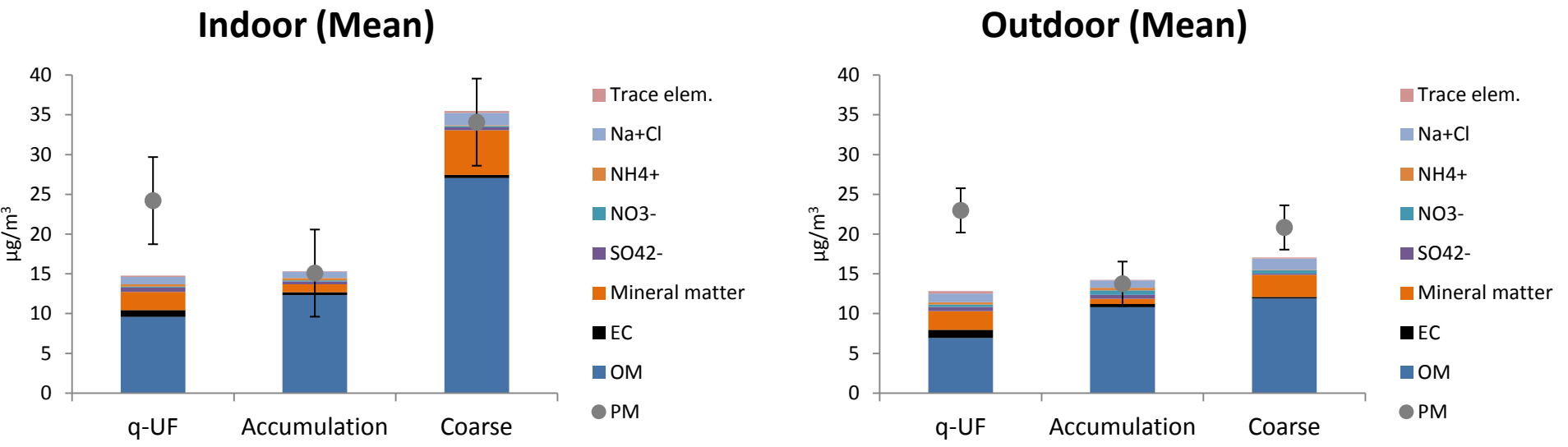
Indoor (Mean)
µg/m³
40
35
30
25
20
15
10
5
0
q-UF
Accumulation
Coarse
Trace elem.
Na+Cl
NH4+
NO3-
SO42-
Mineral matter
EC
OM
PM
Outdoor (Mean)
µg/m³
40
35
30
25
20
15
10
5
0
q-UF
Accumulation
Coarse
Trace elem.
Na+Cl
NH4+
NO3-
SO42-
Mineral matter
EC
OM
PM

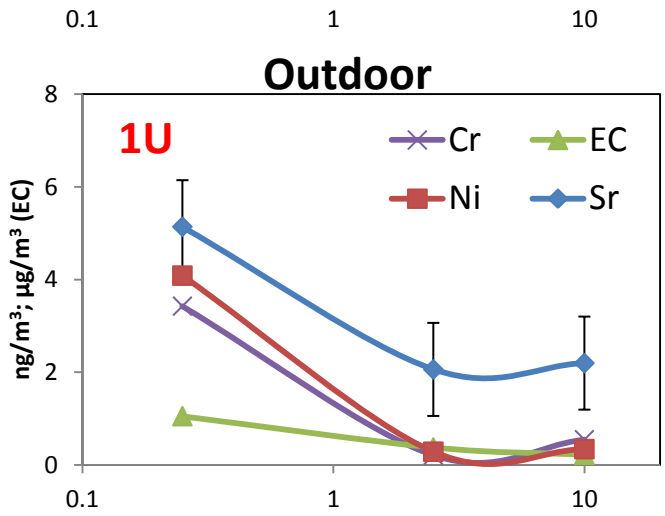
Outdoor
1U
Cr
EC
Ni
Sr
ng/m³; µg/m³ (EC)
0
2
4
6
8
0.1
1
10

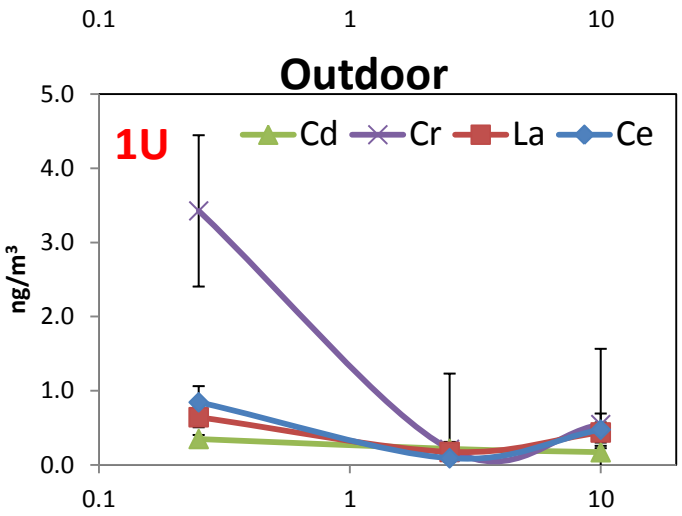
Outdoor
1U
Cd
Cr
La
Ce
ng/m³
0.0
1.0
2.0
3.0
4.0
5.0
0.1
1
10

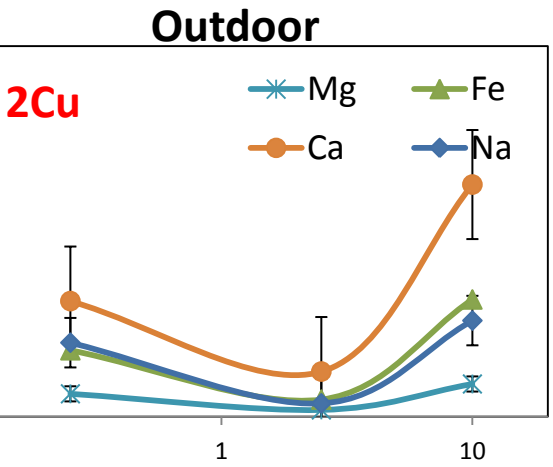
Outdoor
2Cu
Mg
Fe
Ca
Na
1
10

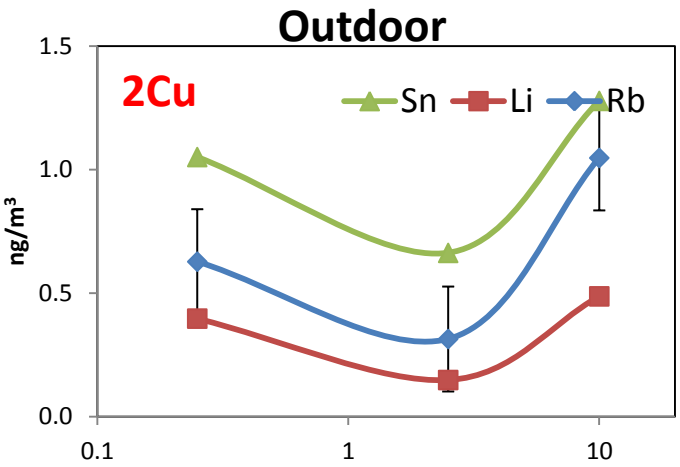
Outdoor
2Cu
Sn
Li
Rb
ng/m³
0.0
0.5
1.0
1.5
0.1
1
10

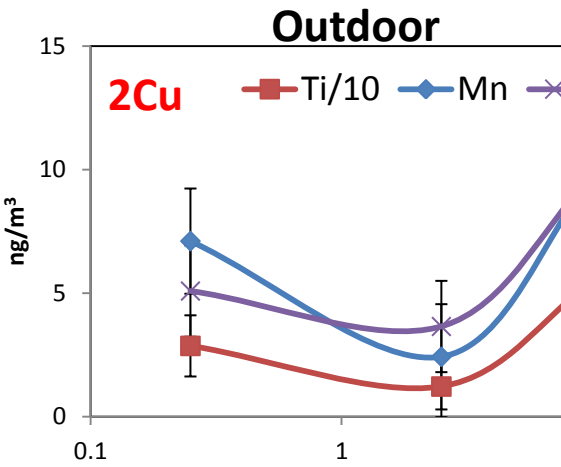
Outdoor
2Cu
Ti/10
Mn
ng/m³
0
5
10
15
0.1
1

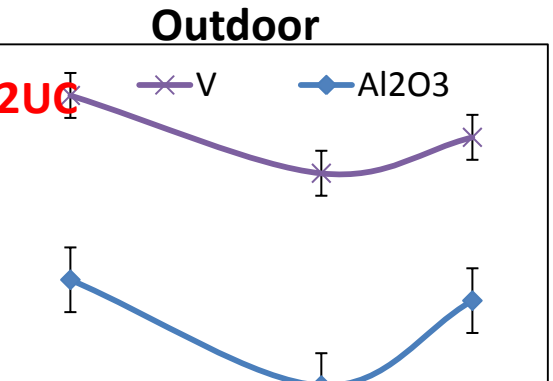
Outdoor
2UC
V
Al2O3

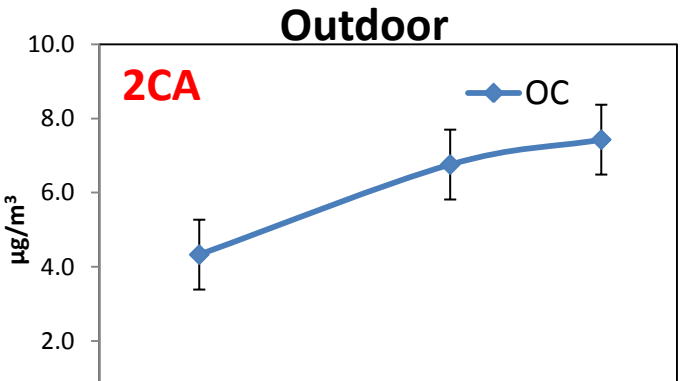
Outdoor
2CA
OC
µg/m³
2.0
4.0
6.0
8.0
10.0

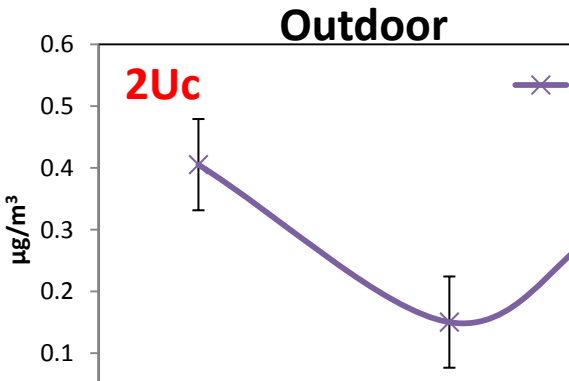
Outdoor
2Uc
µg/m³
0.1
0.2
0.3
0.4
0.5
0.6

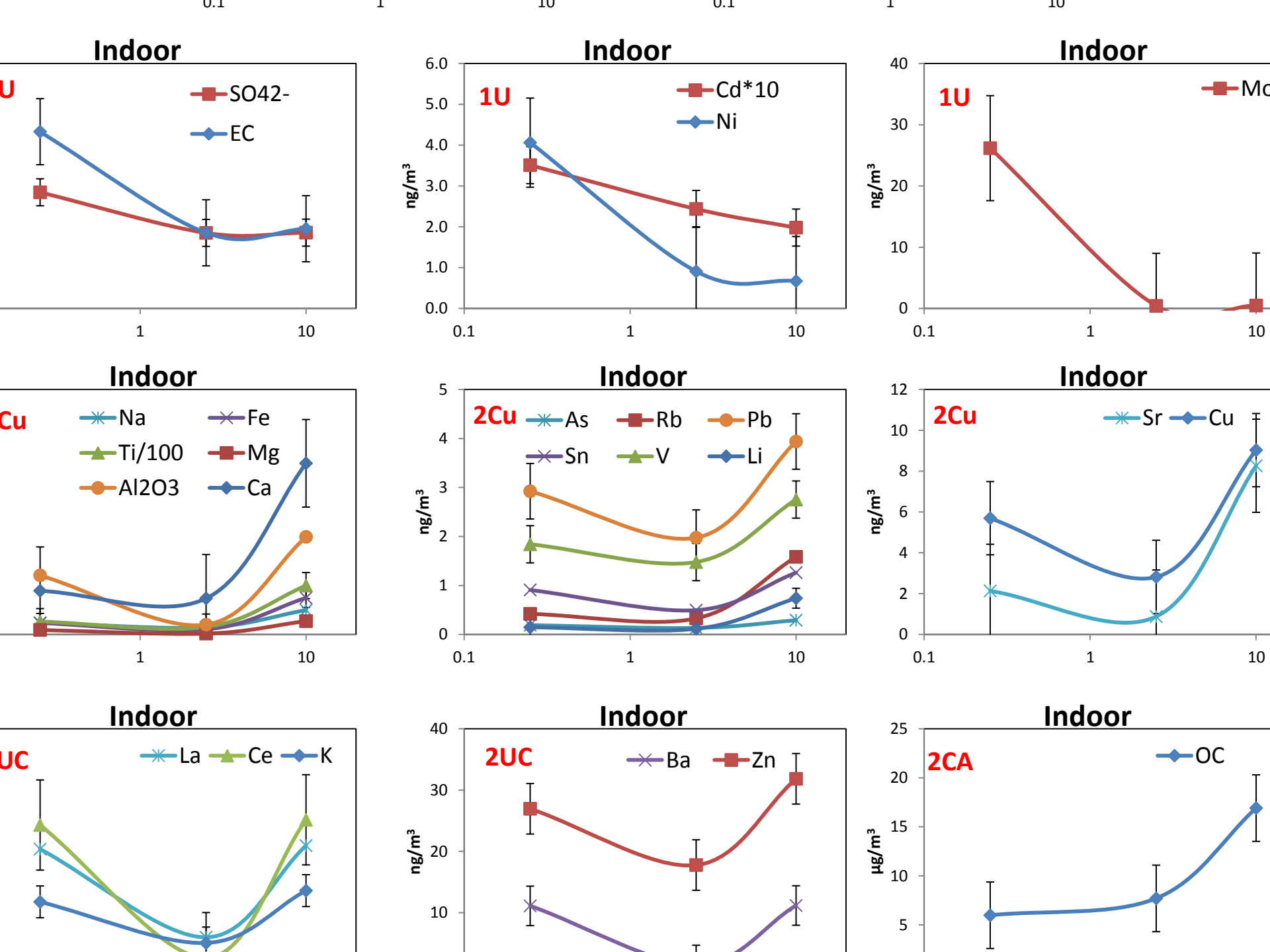
0.1
1
10
0.1
1
10
Indoor
U
SO42-
EC
1
10
Indoor
1U
Cd*10
Ni
ng/m³
6.0
5.0
4.0
3.0
2.0
1.0
0.0
0.1
1
10
Indoor
1U
Mc
ng/m³
40
30
20
10
0
0.1
1
10
Indoor
Cu
Na
Fe
Ti/100
Mg
Al2O3
Ca
1
10
Indoor
2Cu
As
Rb
Pb
Sn
V
Li
ng/m³
5
4
3
2
1
0
0.1
1
10
Indoor
2Cu
Sr
Cu
ng/m³
12
10
8
6
4
2
0
0.1
1
10
Indoor
UC
La
Ce
K
Indoor
2UC
Ba
Zn
ng/m³
40
30
20
10
Indoor
2CA
OC
µg/m³
25
20
15
10
5

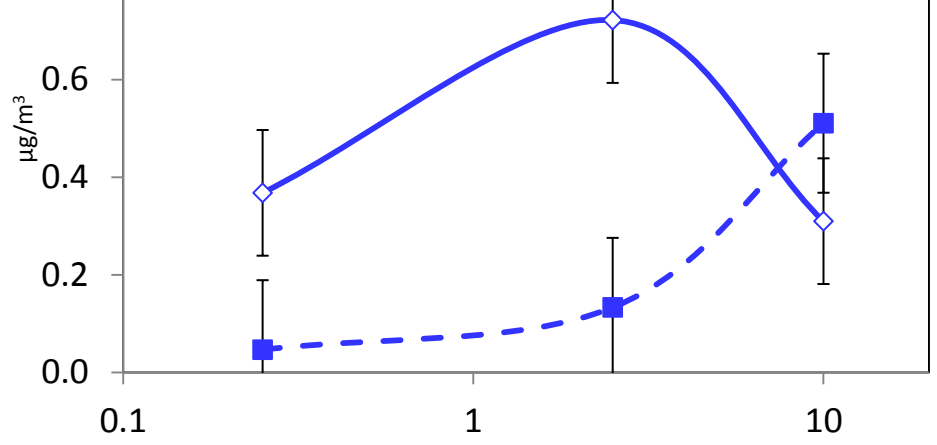

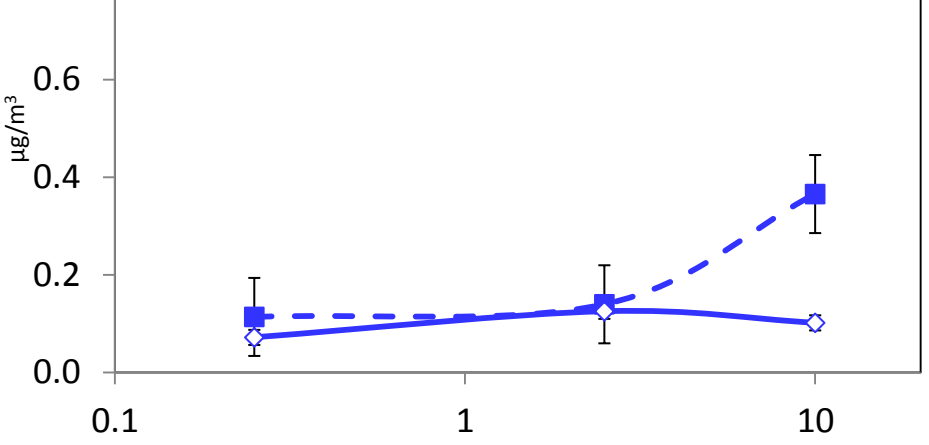

Outdoor SO_4^{2-}

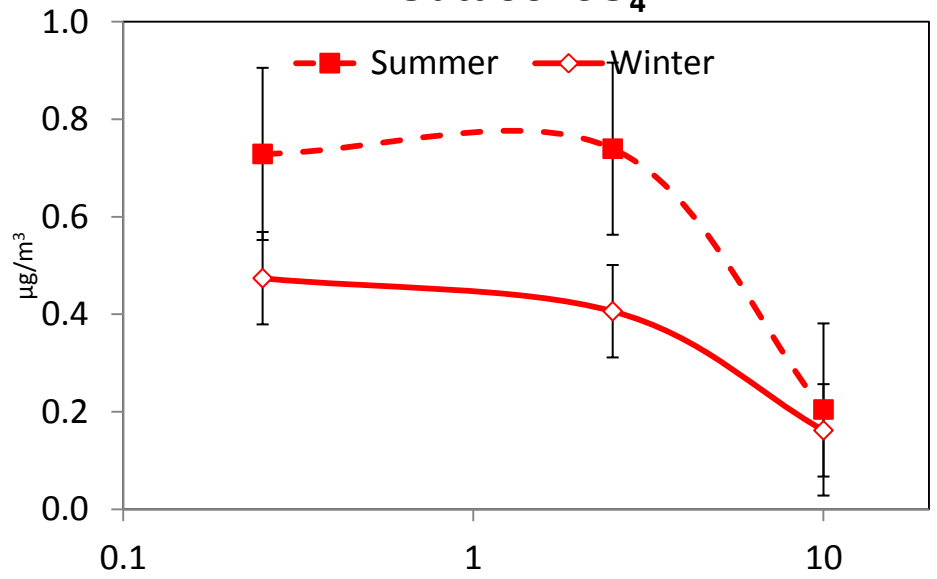

Indoor SO_4^{2-}

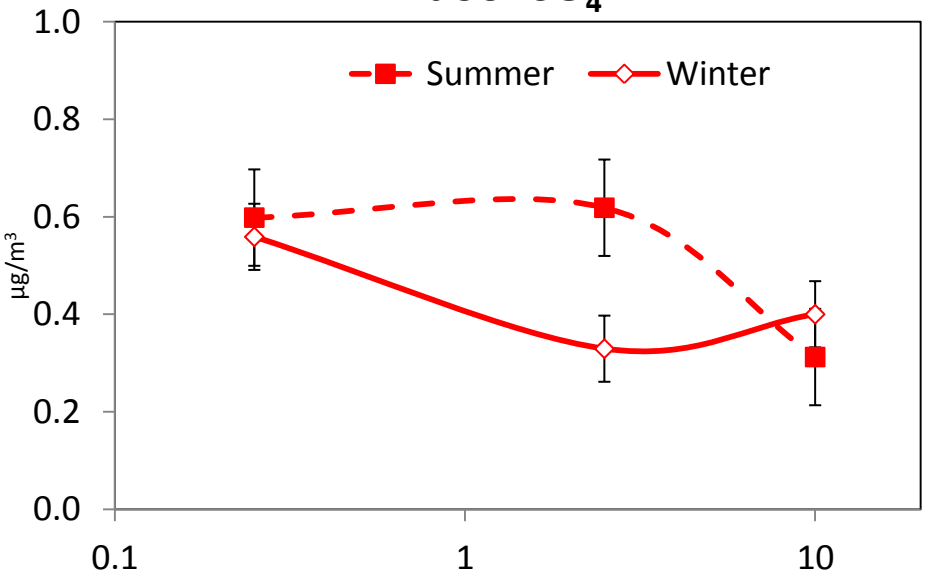

Outdoor OC

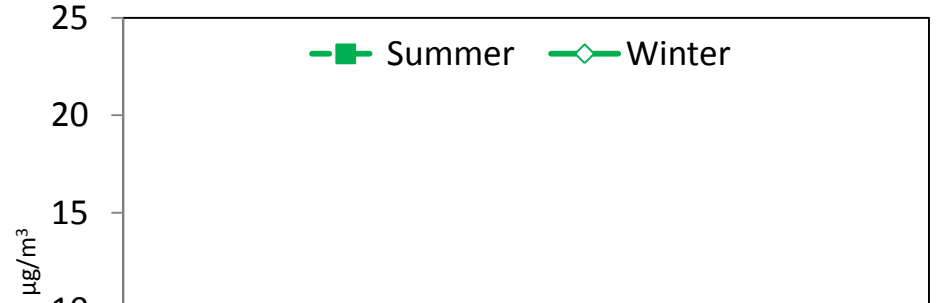

Indoor OC